



Published in final edited form as:

Heart Rhythm. 2006 March ; 3(3): 296–310.

Electrocardiographic imaging of cardiac resynchronization therapy in heart failure: Observation of variable electrophysiologic responses

Ping Jia, PhD^{*}, Charulatha Ramanathan, PhD^{*}, Raja N. Ghanem, PhD^{*}, Kyungmoo Ryu, PhD^{*}, Niraj Varma, MD^{*,†}, and Yoram Rudy, PhD[‡]

^{*}*Cardiac Bioelectricity Research and Training Center, Case Western Reserve University, Cleveland, Ohio*

[†]*University Hospitals of Cleveland, Cleveland, Ohio*

[‡]*Cardiac Bioelectricity and Arrhythmia Center, Washington University in St. Louis, St. Louis, Missouri.*

Abstract

BACKGROUND—Cardiac resynchronization therapy (CRT) for congestive heart failure patients with delayed left ventricular (LV) conduction is clinically beneficial in approximately 70% of patients. Unresolved issues include patient selection, lead placement, and efficacy of LV pacing alone. Being an electrical approach, detailed electrical information during CRT is critical to resolving these issues. However, electrical data from patients have been limited because of the requirement for invasive mapping.

OBJECTIVES—The purpose of this study was to provide observations and insights on the variable electrophysiologic responses of the heart to CRT using electrocardiographic imaging (ECGI).

METHODS—ECGI is a novel modality for noninvasive epicardial mapping. ECGI was conducted in eight patients undergoing CRT during native rhythm and various pacing modes.

RESULTS—In native rhythm (six patients), ventricular activation was heterogeneous, with latest activation in the lateral LV base in three patients and in the anterolateral, midlateral, or inferior LV in the remainder of patients. Anterior LV was susceptible to block and slow conduction. Right ventricular pacing improved electrical synchrony in two of six patients. LV pacing in three of four patients involved fusion with intrinsic excitation resulting in electrical resynchronization similar to biventricular pacing. Although generally electrical synchrony improved significantly with biventricular pacing, it was not always accompanied by clinical benefit.

CONCLUSION—Results suggest that (1) when accompanied by fusion, LV pacing alone can be as effective as biventricular pacing for electrical resynchronization; (2) right ventricular pacing is not effective for resynchronization; and (3) efficacy of CRT depends strongly on the patient-specific electrophysiologic substrate.

Keywords

Heart failure; Resynchronization; Pacing; Imaging; Electrophysiology

Introduction

Delayed ventricular activation,¹ predominantly of the left ventricle (LV), accompanies more than 30% of advanced heart failure cases. Cardiac resynchronization therapy (CRT) using biventricular pacing has been developed to restore synchrony. CRT improves patients' symptoms and echocardiographic measures, and it confers a mortality benefit.² However, many issues related to CRT remain unresolved. For reasons that are not clear, approximately 33% of patients do not respond to CRT [Multicenter InSync Randomized Clinical Evaluation (MIRACLE) trial].³ QRS duration (QRSd) as a criterion for patient selection and assessment of response is weak.^{4,5} LV lead location may be a factor. The incremental benefit of single-site LV pacing alone is unresolved. The electrical consequences of LV pathology have not been examined.

Although improved mechanical performance is the aim of therapy, CRT is an electrical approach that uses pacing and electrophysiologic principles to modify mechanical behavior. The efficacy of the therapy is initially governed by electrical properties and thus may be limited by electrical dysfunction. Hence, failure to achieve resynchronization could be due, in part, to abnormal local electrical properties, such as slow conduction or conduction block, which are likely to be present in patients with LV disease. Therefore, an understanding of the electrophysiologic effects of CRT is essential, requiring high-resolution electrical mapping of ventricular excitation. Until recently, such information could not be obtained noninvasively.

Electrocardiographic imaging (ECGI) is a novel noninvasive imaging modality developed in our laboratory for determining cardiac excitation through noninvasive electrophysiologic epicardial imaging during a single beat. The method has been validated extensively in a human-shaped torso tank containing normal and abnormal canine hearts⁶⁻⁸ and in canine experiments,^{9,10} demonstrating high accuracy in imaging focal activity, infarct substrate, repolarization gradients, and reentry during ventricular tachycardia. ECGI has been applied in humans¹¹ and compared to direct epicardial mapping during open heart surgery¹² and to catheter mapping during ventricular tachycardia.¹³ In humans, ECGI provided images of cardiac activation and repolarization during normal sinus rhythm, conduction disturbances, atrial flutter, and multisite ventricular pacing. A reconstruction accuracy better than 10 mm was consistently obtained in human subjects.¹⁴ Similar to previous studies, we used the ECGI-reconstructed epicardial data in this study to estimate the locations of pacing leads and compared them to the corresponding locations determined from computed tomographic (CT) images. Average accuracy within 10.2 ± 5.1 mm was achieved in locating the pacing sites. With this level of accuracy and extensive validation, ECGI provides a unique tool for noninvasive evaluation of electrophysiologic phenomena, including mechanisms and responses to therapeutic interventions.

In this study, ECGI was applied to eight patients with an implanted CRT device, and ventricular activation during native rhythm and various pacing modes was imaged. Our ultimate goal is to understand the electrophysiologic mechanism(s) that affects responses to CRT and to identify possible use of ECGI in guiding patient selection and lead placement.

This initial study provides preliminary but unique observations on the electrical activity of the heart during CRT and identifies electrical properties that may influence its success as a therapeutic approach. We posed the following hypothesis-driven questions: (1) Is native activation pattern in heart failure patients with left bundle branch block (LBBB) similar in all subjects? (2) Does LV pacing alone evoke similar electrical synchrony as biventricular pacing? (3) Does electrical synchrony correlate with clinical response? (4) Is right ventricular (RV) pacing alone beneficial? These questions were tested in a group of patients with severe LV disease exposed to various pacing modes. The results demonstrated several variables that likely significantly affect pacing efficacy.

Methods

The study evaluated eight heart failure patients (six men and two women; age 72 ± 11 years; New York Heart Association functional class III–IV) with ventricular conduction delay who received CRT through implanted atrial-biventricular pacing device. Six patients had native rhythm with LBBB pattern, one had atrial fibrillation, and one had no underlying rhythm (no AV conduction and no ventricular escape beats) at the time of the study (Table 1). The last two patients were upgraded to biventricular pacing from RV pacing. Optimal atrial-ventricular delay was determined for each patient by Doppler echocardiography (Ritter method¹⁵) during biventricular pacing. All protocols were approved by the Institutional Review Board at University Hospitals of Cleveland, and informed consent was obtained from all patients.

Patients were selected retrospectively at different times (20 days to 15 months) after device implantation. Responders to CRT were identified by echocardiographic evidence of reverse LV remodeling, that is, postimplant improvement of left ventricular ejection fraction (LVEF) and LV internal dimensions at end-diastole and end-systole by examination (Table 1). Specifically, we categorized a patient as responder if two of the three echocardiographic criteria demonstrated more than 10% improvement (LVEF increases and LV internal dimension decreases). Preimplant echocardiographic data were chosen as close as possible to implant date. Postimplant data were acquired as late as possible in the study, to allow time for remodeling following CRT. The earliest postimplant echocardiogram was obtained 6 months after implantation. Additional substrate information from medical history, baseline echocardiography, and nuclear imaging is given in Table 3.

Details of ECGI methodology were described previously.¹¹ In brief, body surface potentials were acquired at 1-ms intervals during the cardiac cycle using a 224-electrode vest and a multichannel mapping system. Body surface potentials were acquired, whenever possible, during RV pacing, LV pacing, biventricular pacing, and native rhythm. A magnetic wand was placed on the left shoulder of the patient, and pacing protocols were performed via a CRT programmer. During all pacing modes, optimal atrial-ventricular delay during biventricular pacing was used. Next, the patient underwent thoracic CT imaging with the vest in position to obtain the heart epicardial geometry and body surface electrode position. Axial resolution of CT was 0.7 mm. Scans were gated at 75% of the ECG R-wave (diastole). This geometric information and the body surface potentials were processed with ECGI algorithms developed in our laboratory to obtain epicardial potentials, electrograms, and activation sequences (isochrones).¹¹ Activation times were determined by the maximal negative slope of the electrograms. Time zero was set at the beginning of QRS for all native rhythm episodes and at ventricular pacing stimuli for all paced episodes.

From the isochrone map, line/region of block was determined if the activation times on its opposite sides differed by more than 50 ms. Activation sequences during intrinsic and paced rhythms were examined, and electrical synchrony was quantified by the index *E_{syn}*, which is the mean activation time difference between lateral RV and LV free walls. The mean activation time was calculated by averaging 50 to 70 activation times distributed over the epicardial surfaces of the lateral walls. RV preexcitation corresponds to negative *E_{syn}* and LV preexcitation to positive *E_{syn}*. *E_{syn}* = 0 indicates interventricular synchrony. Note that *E_{syn}* provides an effective measure of interventricular electrical synchrony, obtained directly from measurements on the heart. In contrast, the widely used QRS_d measure is only a reflection on the body surface of the total duration of ventricular activation and not an index of interventricular synchronization. Table 2 lists mean activation times of the RV and LV during most of the episodes presented in the figures (figures that do not fit into the table format are excluded; however, activation times can be easily estimated from these figures). Table 2 is

intended to facilitate quantitative reading of the maps by providing numerical data on ventricular activation times and interventricular synchrony.

In this study, QRSd was measured by superimposing all body surface ECG recordings and subtracting the earliest onset of the QRS complex from its latest offset among all ECGs. This measurement reflects, to a good approximation, total ventricular activation time. In Table 1, the preimplant QRSd of patients 2 and 6 were obtained from their clinical charts because we could not restore their preimplant rhythms (both patients were implanted with a dual-chamber device).

Results

Native rhythm

Native rhythm was imaged in six patients by inactivating the CRT device. Four representative maps are shown in Figure 1. ECG was similar to the preimplant ECG, indicating similar activation sequences. In all six patients, RV epicardial activation started from RV breakthrough 29 ± 7 ms after onset of body surface QRS. This is delayed relative to that in normal young adults.¹⁶ Epicardial activation spread radially from the RV breakthrough site, with latest activation of the RV at basal RV or anterior/inferior paraseptal region (mean RV activation times are provided in Table 2). The duration for entire RV activation after RV breakthrough was 25 ± 12 ms. The RV activation pattern was consistent with that imaged in normal hearts using ECGI.¹⁶ LV activation patterns were diverse and consistent with LBBB. In patients 4, 7, and 8, LV epicardial activation started from the septoapical region, spreading laterally and ending at the lateral or posterolateral base (Figure 1A; see also Figures 4A and 4B, top). In patient 5, the activation wavefront spread superiorly from inferior LV rather than from the apical region, ending at the midanterolateral wall (Figure 1B). In these four patients, activation that crossed the septum from RV was prevented from spreading further into the LV by an anterior line(s)/region(s) of block (black). It reached the lateral wall by way of either apical or inferior LV. A similar activation pattern was observed and termed a *U-shaped pattern* by Auricchio et al¹⁷ using endocardial mapping. Some line(s)/region(s) of block shifted to other locations or were absent during subsequent pacing protocols, indicating the functional nature of the block. Others did not change with pacing, suggesting fixed anatomic block. Table 3 provides substrate information and line of block location for each patient. Patient 1 had LV breakthrough at 49 ms (Figure 1C, left lateral view). Wavefronts advancing from apical, inferior, and superior LV all contributed to overall LV activation, which ended at the posterolateral wall. In patient 3 (Figure 1D), activation could not spread through inferior LV. Instead, it slowly propagated across the septum from RV and reached the LV lateral and posterior walls by spreading inferoposteriorly from anterior LV. Latest activation was at the inferoposterior base.

Activation during RV pacing

RV endocardial pacing sites were located in the low apical region, except in patients 1 and 6 who had a midseptal lead placement. Pacing produced very different RV activation sequences (Figure 2) compared to native rhythm. In most cases, RV activation was much slower during pacing (during RV pacing, the duration of RV epicardial activation after RV breakthrough was 51 ± 15 ms vs 25 ± 12 ms in native rhythm), presumably because of lacking or limited conduction system involvement during a paced beat compared to native rhythm. Patient 3 (Figure 2D) was an exception due to early fusion of paced and intrinsic excitation that accelerated RV activation relative to native excitation. In the LV, RV pacing generated similar activation sequences to that of native rhythm, with some differences on anterior LV. In particular, lines of block were different compared to those during the corresponding native

rhythm. RV pacing improved electrical synchrony in patient 5 (Figure 2) but failed to improve synchrony in patients 1, 3, and 7.

Epicardial activation during biventricular pacing

Considerable differences were detected among patients in terms of activation patterns and electrical synchrony during biventricular pacing as evaluated by ECGI. Among responders (patients 1, 3, and 5) and nonresponders (patients 2, 4, 6, 7, and 8), each patient had a unique pattern as presented in the following.

Figure 3 shows epicardial activation during both native rhythm and biventricular pacing in two patients (5 and 3, both responders). The LV pacing lead of patient 5 was located at the lateral wall (Figure 3A, bottom). Activation spread from the pacing site and ended locally at basal LV 110 ms after pacing. On the anterior LV, activation was blocked by a line of block, similar to that during the native beat (Figure 3A, top). Latest activation occurred at anterior LV, immediately adjacent to the line of block, at 138 ms. Compared to native rhythm, RV and the major part of LV were much more synchronized electrically (Esyn improved from -113 to 20 ms). Patient 3 had an anterior LV lead and a line of block located anterolaterally (Figure 3B). Activation pivoted around this block and ended at lateral basal LV at 117 ms. Both patients responded to CRT as judged by improvement of postimplant echocardiographic parameters (patient 3: LVEF increased from 25%–30% to 30%–40%, LV internal dimension at end-systole decreased by 25%; patient 5: LVEF increased from 25% to 40%, LV internal dimension decreased by 10%).

Patient 8 had a lateral LV lead (Figure 4A). The RV and LV lateral walls were electrically more synchronized (Esyn improved from -56 to -26 ms), although QRSd did not shorten with biventricular pacing (QRSd = 130 ms in native rhythm and 140 ms in biventricular pacing). Due to interference of many lines of block, latest activation occurred in anterior LV at 132 ms. This patient was a nonresponder despite electrical synchronization of RV and lateral LV. Figure 4B shows patient 4, who had an anterior LV pacing lead. LV lateral wall activation was slowed relative to native rhythm and took twice as long to reach the basal LV. This region of slow conduction only appeared during the paced beat, indicating dependence on the geometry and direction of the wavefront relative to the myocardial structure. This patient also was a nonresponder.

Figure 5 shows two patients (1 and 7) with lateral LV leads. The activation patterns were similar to those of patients 5 and 8. RV and lateral LV wall were synchronized electrically. Clinically, patient 1 was a “slow” responder with late (>6 months) improvement. Echocardiographic LV remodeling was observed to occur 12 months postimplant. Patient 7 was a nonresponder.

Patient 6 was a unique case in this study. She initially was implanted with a device that allowed only simultaneous biventricular pacing, but she did not improve and remained a nonresponder. Her 12-lead ECG during biventricular pacing was the same as during RV pacing. The device was upgraded to a newer version that allowed pacing the two ventricles separately with a preset time delay. Imaging during RV, LV, biventricular simultaneous, and biventricular sequential pacing is shown in Figure 6. During biventricular simultaneous pacing, RV breakthrough was 30 ms earlier than LV breakthrough. Comparing RV and biventricular pacing (Figures 6A and 6C), the LV lead was located at an area where activation from RV pacing arrived at approximately the same time as the LV pacing breakthrough. Consequently, LV pacing had no effect on the activation sequence, which explains why the ECG was the same for RV and biventricular pacing modes. With 80-ms preexcitation of LV relative to RV, activation was similar to that during LV pacing alone, with RV activation advanced by approximately 30 ms due to the additional RV pacing (Figure 6D). A line of block across the LV lateral free wall was present consistently over all pacing modes. It prevented any anterior activation from

propagating inferiorly to the midlateral region. This region was activated by a wavefront propagating superiorly from inferior LV (for RV or biventricular simultaneous pacing, Figures 6A and 6C), or possibly by an intramural wavefront (for LV or biventricular sequential pacing, Figures 6B and 6D). In addition, during LV or biventricular sequential pacing, a line of block between lateral and inferior LV prevented lateral activation from propagating inferiorly. This was a line of functional unidirectional block, as it allowed wavefront propagation in the reverse direction in the other two pacing modes. Because of these complex barriers, global activation could propagate around the heart only in a counterclockwise fashion. Inferior LV could be activated only by wavefront spreading from the RV. In terms of electrical synchrony, biventricular sequential pacing was better than biventricular simultaneous pacing.

LV pacing and fusion beats

With optimal atrial-ventricular delay, three of four patients with AV conduction in whom the device was programmed for LV pacing alone showed fusion between intrinsic excitation and the LV paced beat. Depending on the relative length of the PR interval and optimal atrial-ventricular delay, the degree of fusion varied. In patient 5, we captured a series of LV paced beats with increasing degree of fusion (resulting from progressively varied atrial-ventricular delay). Figure 7A shows pure LV paced activation without fusion, at atrial-ventricular delay ≤ 0 . Figures 7B through 7D show activation for the same LV pacing protocol with increasing degree of fusion due to increasing atrial-ventricular delay; intrinsic excitation couples to the paced beat progressively earlier, with increasing contribution to ventricular activation. Fusion significantly influenced the degree of electrical synchrony during LV pacing, with E_{syn} improving as fusion increases (Figure 7D).

Discussion

The unique capability of ECGI for noninvasive epicardial mapping was used to determine activation sequences during pacing in a group of eight patients undergoing CRT with the following observations. (1) Activation sequences during native rhythm were heterogeneous among individuals. (2) RV pacing was not effective in resynchronization in most patients. (3) LV pacing often generated similar electrical synchrony as biventricular pacing due to fusion. (4) Anterior LV pacing was less effective than lateral pacing in synchronizing the LV due to severe anterior conduction disturbances. (5) LV pacing efficacy was influenced by pacing lead position relative to the properties of the electrophysiologic substrate.

ECGI in this series provided important insights. Patients with heart failure and LBBB ECG pattern did not constitute a homogeneous group, as they displayed (during native rhythm) a wide range of electrical activation patterns, with regions of delayed and/or absent conduction, reflecting varied LV pathology. Response to pacing from either the RV or LV was similarly disparate, and overall LV activation and RV-LV electrical synchrony depended on the sites paced, adjacent regions of pathology, and development of pacing site-dependent functional lines of block. This suggests that highly heterogeneous LV substrates and difficult to predict electrical responses to pacing may account for the highly varied clinical responses to CRT.

Native rhythm

Activation patterns in heart failure patients with LBBB were studied by several groups using endocardial mapping.^{17,18} Consistent with these studies, we observed heterogeneous LBBB activation patterns, with LV activation delayed (mean delay 90 ms) relative to RV activation. Note that, in normal adults, average LV epicardial activation time is delayed by <40 ms relative to that of RV epicardium.¹⁶ As suggested by the data in Table 3, there is no obvious correlation between regions with motion abnormalities (or scarring) and the locations of lines of block detected by ECGI. This finding demonstrates the complex relationships among structural,

mechanical, and electrical substrates in the heart; it is consistent with many studies showing functional lines of block and areas of slow conduction that are not directly related to structural or mechanical alterations in hearts with structural abnormalities. The lack of correlation highlights the need to characterize separately the electrical substrate using methods such as ECGI. Most patients had line(s)/region(s) of block in anterior LV that was functional or anatomic. The block prevented RV activation from crossing directly to the LV and usually resulted in a U-shaped activation pattern that circumvented the block via apical or inferior LV. The latest activation occurred most often at lateral LV base, although late activation also was observed in anterolateral, midlateral, or inferior LV walls. In previous studies, the latest LV region of mechanical activation was identified as the optimal pacing site for CRT,¹⁹⁻²¹ and tissue Doppler imaging was used to locate this region.^{18,20} Using tissue Doppler imaging and endocardial mapping, correlation was found between the region of latest electrical and mechanical activation in LV.¹⁸ The ability of ECGI to determine the region of late electrical activation noninvasively suggests that it could be used to guide lead placement for CRT. An invasive study by Tse et al²² suggested that the percentage area of LV that displayed late activation times could predict acute responses during LV stimulation. ECGI certainly could provide such information noninvasively to facilitate proper patient selection for CRT based on this criterion. Our ECGI maps show relatively normal RV activation, indicating that although LV myocardium and left bundle branch are severely damaged, the right bundle and RV myocardium preserve relatively normal function.

RV pacing, LV pacing, and fusion

In the six patients who had native rhythm (patients 1, 3, 4, 5, 7, and 8), RV pacing improved native electrical synchrony in two patients (5 and 8) but not in the remaining four patients. Whether RV pacing improves electrical synchrony might depend on the interaction and timing of the paced and intrinsic activation. This, in turn, depends on the relative conduction velocity of the intrinsic activation which uses the conduction system, and cell-to-cell propagation of the paced activation, a property that depends on the substrate and, therefore, is patient specific. This electrical observation is consistent with the variable clinical outcome of RV pacing, where both improved or deteriorated hemodynamic function is observed in a patient-specific manner.²³ During LV pacing beats, fusion plays an important role in electrical synchrony. At optimal atrial-ventricular delay, three of four patients (1, 3, and 5) showed significant fusion and a similar level of electrical synchrony as during biventricular pacing.

Electrical resynchronization and clinical response

We observed that electrical activation of the lateral LV wall was advanced significantly by biventricular pacing, improving electrical synchrony in most patients, including the three responders (1, 3, and 5) and three of the five nonresponders (6, 7, and 8). The absence of response in three of these patients suggests that electrical synchrony does not always correlate to clinical improvement. The lack of correlation could be due to heterogeneous mechanical response to electrical resynchronization in different patients. The inconsistency of the mechanical–electrical relationship was observed in a canine study in which mechanical synchrony occurred in response to various, highly different electrical activation sequences.²⁴ Systematic investigation of the relationship between electrical and mechanical synchrony is needed to explain this property. Future studies using ECGI, which provides the required electrical information, in combination with noninvasive modalities for assessing cardiac mechanics, such as tissue Doppler imaging or magnetic resonance imaging, could provide important insights into this phenomenon.

QRSd is used as a criterion for patient selection, but QRS narrowing in response to CRT has proved to be a disappointing index of electrical synchrony. ECGI activation maps demonstrate the limitations of QRSd in this context. For example, patient 5 clearly improved synchrony

during RV pacing, with Esyn improving from -113 ms (native rhythm) to -61 ms (compare Figures 1B and 2B). However, QRSd increased slightly (from 180 to 190 ms). QRSd during RV pacing (Figure 2B) is skewed by a long activation delay in a small region near the pacing site that has minimal effect on global electrical synchrony. Therefore, despite improvement of global synchrony, QRSd remains prolonged and does not reflect successful electrical resynchronization. Another example is patient 8 (Figure 4A), in whom biventricular pacing improved synchrony without shortening QRSd. Therefore, QRSd does not necessarily decrease as electrical synchronization increases. These observations help to explain the lack of correlation between electrical synchronization (Esyn) and QRSd (Table 2).

Lead placement

Three of five nonresponders (2, 4, and 6) did not achieve electrical synchrony during simultaneous biventricular pacing. Their electrical activation pattern during biventricular pacing showed significant RV preexcitation, similar to that of unpaced LBBB. All three patients had anterior LV leads. Butter et al¹⁹ reported superior clinical benefit with lateral lead placement compared to anterior placement. Four of our patients (2, 3, 4, and 6) had an anterior LV lead (high anterolateral vein in patients 2, 3, and 6; anterior interventricular vein in patient 4). In three of these four patients (2, 4, and 6), simultaneous biventricular pacing failed to improve electrical synchrony. In the remaining patient (3), electrical synchrony improved modestly. The activation pattern remained RV preexcitation but was different from the other three patients; the line of block was relatively short and the anterior activation front propagated to the lateral LV by pivoting around it without major conduction delays. This provides an example of the dependence of pacing efficacy on the electrical substrate adjacent to the pacing lead. In contrast, all four patients (1, 5, 7, and 8) with lateral leads achieved electrical synchrony. The inefficacy of anterior leads in activating the LV probably is due to the high likelihood of regions of conduction block and slow conduction (anatomic and functional) in the anterolateral aspects that interfere with propagation from the anterior to the lateral wall. In fact, in two of these patients (2 and 4), pacing from anterior LV influenced RV activation more than LV activation.

In patient 2, who had extensive anterior and anterolateral LV scarring, the excitation generated by the anteriorly located LV lead activated the RV but failed to propagate to the LV because of an anterior line of block. Therefore, the impact of LV pacing was negligible. Serial postimplant echocardiography demonstrated progressive deterioration with dilatation and diminishing LVEF, until the patient died of heart failure 9 months later. Despite this result, the patient improved two functional classes (from New York Heart Association class IV to II) within 4 weeks postimplantation. This was the only patient in whom we found a major discrepancy between clinical effects of CRT (improved) and electrical (ECGI) and echocardiographic evidence of benefit (absent). This may be accounted for by a placebo-like effect, which is well recognized in device trials, including MIRACLE.

These observations suggest that determination of optimal LV lead placement should consider not only the sequence of activation (i.e., pacing from the region of most delayed activation to maximize synchrony) but also electrical properties of the substrate, especially when disease is advanced. Presence of inexcitable tissue, regions of conduction block, or areas of slow conduction and their location relative to the pacing lead have an important effect on pacing efficiency and outcome. Invasive catheter mapping has been found useful in locating less abnormal regions with relatively fast conduction that are suitable for lead placement.²⁵ ECGI can provide noninvasively similar information for guiding lead placement. For example, in patient 6 (Figure 6), two lateral lines of block (one unidirectional) formed a complex barrier for electrical activation, forcing it to propagate in a counterclockwise direction regardless of the pacing mode. For this patient, a more inferior lead location could be advantageous by

helping to avoid the lines of block. The current coronary venous approach of implanting LV leads limits the accessible locations for lead placement. However, implantation techniques are constantly advancing, including placement of epicardial LV leads, making substrate-dependent, individualized lead placement a conceivable future strategy.

Study limitations

ECGI, as a novel imaging research tool, is limited in terms of its data processing automation and speed, which precludes large population clinical trials at this time. This initial study of electrical activation in CRT was limited to eight patients (three responders and five nonresponders). It provided important observations and mechanistic insights on the electrical processes during CRT. A large-scale trial in identified subgroups within the CRT-treated population, to address the various electrical abnormalities generated by heterogeneous disease patterns, will require a more clinically developed ECGI system. Another limitation of ECGI is that, similar to intraoperative mapping, it obtains data on the epicardial surface of the heart but not in the myocardial volume or septum. As a result, early activation times prior to epicardial breakthrough are not accounted for when Esyn is computed. The lack of septal information precludes using Esyn to evaluate intraventricular electrical synchrony. As shown by Bordachar et al,²⁶ intraventricular mechanical synchrony may correlate better with hemodynamic improvement than interventricular mechanical synchrony. Also, ECGI spatial resolution limits exact separation of LV and RV activation to within 10 mm, which could affect Esyn. It is important to recognize, however, that Esyn is not used here as an absolute physiologic measure of activation synchrony in the heart; rather, it is an index obtained from the heart surface that provides quantitative measure of interventricular synchrony. It is used in this study as a relative measure to compare the levels of synchrony during different activation sequences (native rhythm and various pacing modes) in the same patient. Used as a relative measure of synchrony, Esyn is self-consistent.

Acknowledgments

We thank Paul Kohanski, Leslie Ciancibello, Sheila Shaffer, and Elena DuPont for assistance in pacing and CT data acquisition and transfer.

The study was supported by Merit Award R37-HL-33343 and Grant R01-HL-49054 from the National Heart, Lung, and Blood Institute of the National Institutes of Health to Dr. Rudy. Dr. Rudy is the Fred Saigh Distinguished Professor at Washington University in St. Louis. Drs. Jia and Ramanathan are employees and stockholders of Cardioinsight, Inc., a company that plans to commercialize electrocardiographic imaging as a clinical tool. Dr. Rudy is a coinventor of the ECGI technology.

References

1. Farwell D, Patel NR, Hall A, Ralph S, Sulke AN. How many people with heart failure are appropriate for biventricular resynchronization? *Eur Heart J* 2000;21:1246–1250. [PubMed: 10924314]
2. Cleland JGF, Daubert J-C, Erdmann E, Freemantle N, Gras D, Kappenberger L, Tavazzi L. the Cardiac Resynchronization-Heart Failure (CARE-HF) Study Investigators. The effect of cardiac resynchronization on morbidity and mortality in heart failure. *N Engl J Med* 2005;352:1539–1549. [PubMed: 15753115]
3. Abraham WT, Fisher WG, Smith AL, Delurgio DB, Leon AR, Loh E, Kocovic DZ, Packer M, Clavell AL, Hayes DL, Ellestad M, Messenger J, Trupp RJ, Underwood J, Pickering F, Truex C, McAtee P. Cardiac resynchronization in chronic heart failure. *N Engl J Med* 2002;346:1845–1853. [PubMed: 12063368]
4. Auricchio A, Stellbrink C, Block M, Sack S, Vogt J, Bakker P, Klein H, Kramer A, Ding J, Salo R, Tockman B, Pochet T, Spinelli J. Effect of pacing chamber and atrioventricular delay on acute systolic function of paced patients with congestive heart failure. The Pacing Therapies for Congestive Heart Failure Study Group. The Guidant Congestive Heart Failure Research Group. *Circulation* 1999;99:2993–3001. [PubMed: 10368116]

5. Nelson GS, Curry CW, Wyman BT, Kramer A, Declerck J, Talbot M, Douglas MR, Berger RD, McVeigh ER, Kass DA. Predictors of systolic augmentation from left ventricular preexcitation in patients with dilated cardiomyopathy and intraventricular conduction delay. *Circulation* 2000;101:2703–2709. [PubMed: 10851207]
6. Oster HS, Taccardi B, Lux RL, Ershler PR, Rudy Y. Noninvasive electrocardiographic imaging: reconstruction of epicardial potentials, electrograms, and isochrones and localization of single and multiple electrocardiac events. *Circulation* 1997;96:1012–1024. [PubMed: 9264513]
7. Burnes JE, Taccardi B, MacLeod RS, Rudy Y. Noninvasive ECG imaging of electrophysiologically abnormal substrates in infarcted hearts: a model study. *Circulation* 2000;101:533–540. [PubMed: 10662751]
8. Burnes JE, Taccardi B, E. PR, Rudy Y. Noninvasive electrocardiogram imaging of substrate and intramural ventricular tachycardia in infarcted hearts. *J Am Coll Cardiol* 2001;38:2071–2078. [PubMed: 11738317]
9. Burnes JE, Ghanem RN, Waldo AL, Rudy Y. Imaging dispersion of myocardial repolarization, I: comparison of body-surface and epicardial measures. *Circulation* 2001;104:1299–1305. [PubMed: 11551883]
10. Ghanem RN, Burnes JE, Waldo AL, Rudy Y. Imaging dispersion of myocardial repolarization, II: noninvasive reconstruction of epicardial measures. *Circulation* 2001;104:1306–1312. [PubMed: 11551884]
11. Ramanathan C, Ghanem RN, Jia P, Ryu K, Rudy Y. Noninvasive electrocardiographic imaging for cardiac electrophysiology and arrhythmia. *Nat Med* 2004;10:422–428. [PubMed: 15034569]
12. Ghanem R, Ramanathan C, Jia P, Ryu K, Markowitz A, Rudy Y. Noninvasive electrocardiographic imaging (ECGI): comparison to intraoperative mapping in patients. *Heart Rhythm* 2005;2:339–354. [PubMed: 15851333]
13. Intini A, Goldstein RN, Jia P, Ramanathan C, Ryu K, Giannattasio B, Gilkeson R, Stambler BS, Brugada P, Stevenson WG, Rudy Y, Waldo AL. Electrocardiographic imaging (ECGI), a novel diagnostic modality used for mapping of focal left ventricular tachycardia in a young athlete. *Heart Rhythm* 2005;2:1250–1252. [PubMed: 16253916]
14. Ghosh S, Rudy Y. Accuracy of quadratic versus linear interpolation in noninvasive electrocardiographic imaging (ECGI). *Ann Biom Eng* 2005;33:1187–1201.
15. Ritter P, Padeletti L, Gillio-Meina L, Gaggini G. Determination of the optimal atrioventricular delay in DDD pacing. Comparison between echo and peak endocardial acceleration measurements. *Europace* 1999;1:126–130. [PubMed: 11228855]
16. Ramanathan C, Jia P, Ghanem R, Ryu K, Rudy Y. Noninvasive electrocardiographic imaging (ECGI) of normal activation and repolarization of the human heart (abstr). *Pacing Clin Electrophysiol* 2003;26(pt II):II-995.
17. Auricchio A, Fantoni C, Regoli F, Carbucicchio C, Goette A, Geller C, Kloss M, Klein H. Characterization of left ventricular activation in patients with heart failure and left bundle-branch block. *Circulation* 2004;109:1133–1139. [PubMed: 14993135]
18. Fung JW, Yu CM, Yip G, Zhang Y, Chan H, Kum CC, Sanderson JE. Variable left ventricular activation pattern in patients with heart failure and left bundle branch block. *Heart (Br Card Soc)* 2004;90:17–19.
19. Butter C, Auricchio A, Stellbrink C, Fleck E, Ding J, Yu Y, Huvelle E, Spinelli J. Pacing Therapy for Chronic Heart Failure IISG. Effect of resynchronization therapy stimulation site on the systolic function of heart failure patients. *Circulation* 2001;104:3026–3029. [PubMed: 11748094]
20. Ansalone G, Giannantoni P, Ricci R, Trambaiolo P, Fedele F, Santini M. Doppler myocardial imaging to evaluate the effectiveness of pacing sites in patients receiving biventricular pacing. *J Am Coll Cardiol* 2002;39:489–499. [PubMed: 11823088]
21. Kass DA. Ventricular resynchronization: pathophysiology and identification of responders. *Rev Cardiovasc Med* 2003;4(suppl 2):S3–S13. [PubMed: 12776008]
22. Tse H-F, Lee KL, Wan S-H, Yu Y, Hoersch W, Pastore J, Zhu Q, Kenknight B, Spinelli J, Lau C-P. Area of left ventricular regional conduction delay and preserved myocardium predict responses to cardiac resynchronization therapy. *J Cardiovasc Electrophysiol* 2005;16:690–695. [PubMed: 16050824]

23. Yu Y, Kramer A, Spinelli J, Ding J, Hoersch W, Auricchio A. Biventricular mechanical asynchrony predicts hemodynamic effect of uniand biventricular pacing. *Am J Physiol Heart Circ Physiol* 2003;285:H2788–H2796. [PubMed: 14613916]
24. Leclercq C, Faris O, Tunin R, Johnson J, Kato R, Evans F, Spinelli J, Halperin H, McVeigh E, Kass DA. Systolic improvement and mechanical resynchronization does not require electrical synchrony in the dilated failing heart with left bundle-branch block. *Circulation* 2002;106:1760–1763. [PubMed: 12356626]
25. Lambiase PD, Rinaldi A, Hauck J, Mobb M, Elliott D, Mohammad S, Gill JS, Bucknall CA. Non-contact left ventricular endocardial mapping in cardiac resynchronisation therapy. *Heart (Br Card Soc)* 2004;90:44–51.
26. Bordachar P, Lafitte S, Reuter S, Sanders P, Jaïs P, Haïssaguerre M, Roudaut R, Garrigue S, Clementy J. Echocardiographic parameters of ventricular dyssynchrony validation in patients with heart failure using sequential biventricular pacing. *J Am Coll Cardiol* 2004;44:2157–2165. [PubMed: 15582313]

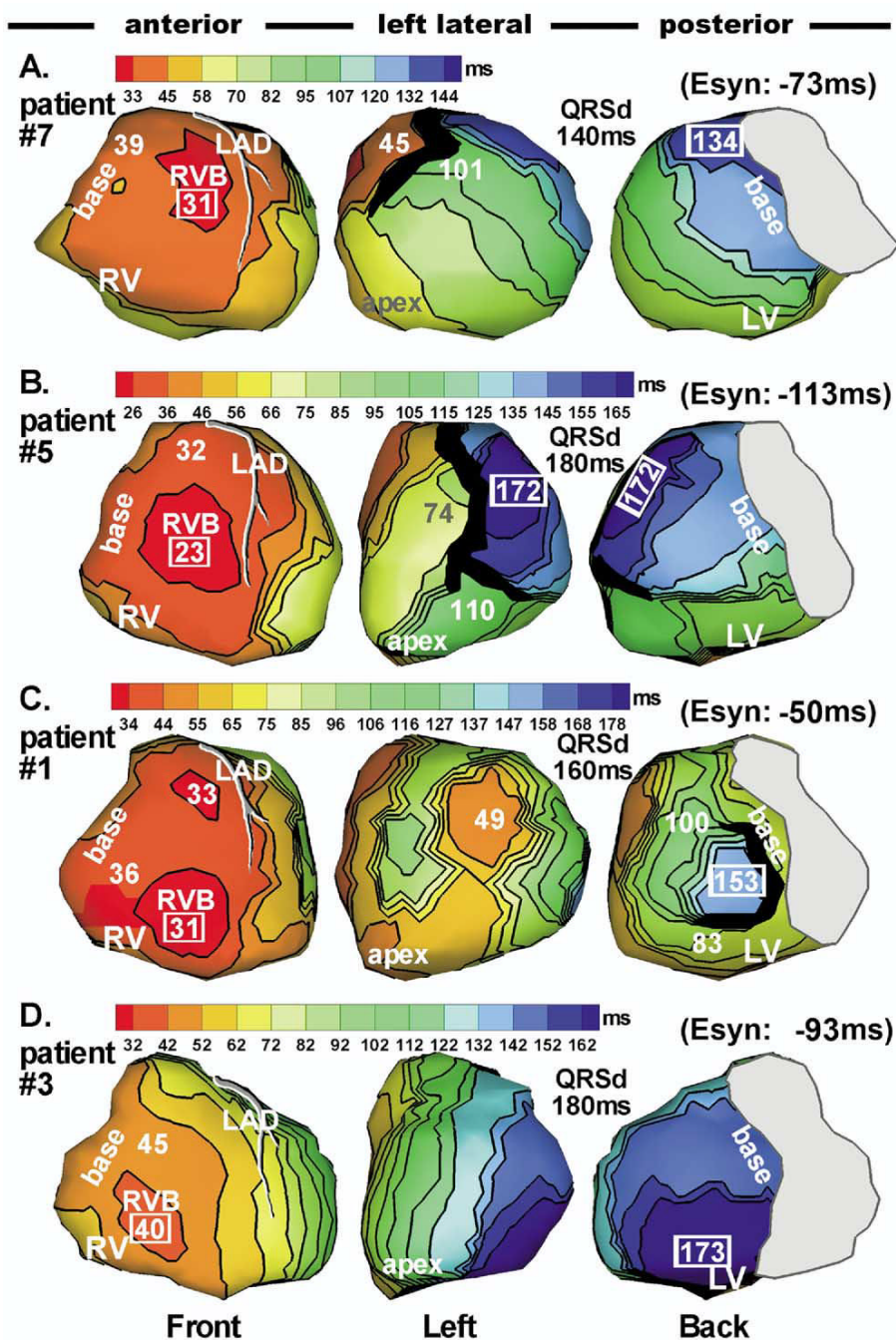


Figure 1. Epicardial isochrone maps during native rhythm in four representative patients. Epicardial surfaces of both ventricles are displayed in three views: anterior, left lateral, and posterior. There is overlap between adjacent views. Left anterior descending (LAD) coronary artery is shown. The approximate valve region is covered by gray. Thick black markings indicate line/region of conduction block. All isochrone maps show sequential ventricular activation of right ventricle (RV) followed by a much delayed left ventricular (LV) activation, indicating left bundle branch block (LBBB). Several LV activation patterns were identified. A: Apical to lateral basal conduction. B: Inferior to anterolateral conduction. C: Combined activation from apical, inferior, and superior LV. D: Anterior to inferoposterior conduction. Activation times

(in milliseconds) of selected regions, such as RV breakthrough, latest activation, and sites adjacent to block regions, are indicated on the map. Earliest and latest ventricular activation times are indicated by framed numbers. All activation times are given with respect to QRS onset. E_{syn} = electrical synchrony index (smaller absolute value corresponds to greater synchrony); QRS_d = QRS duration.

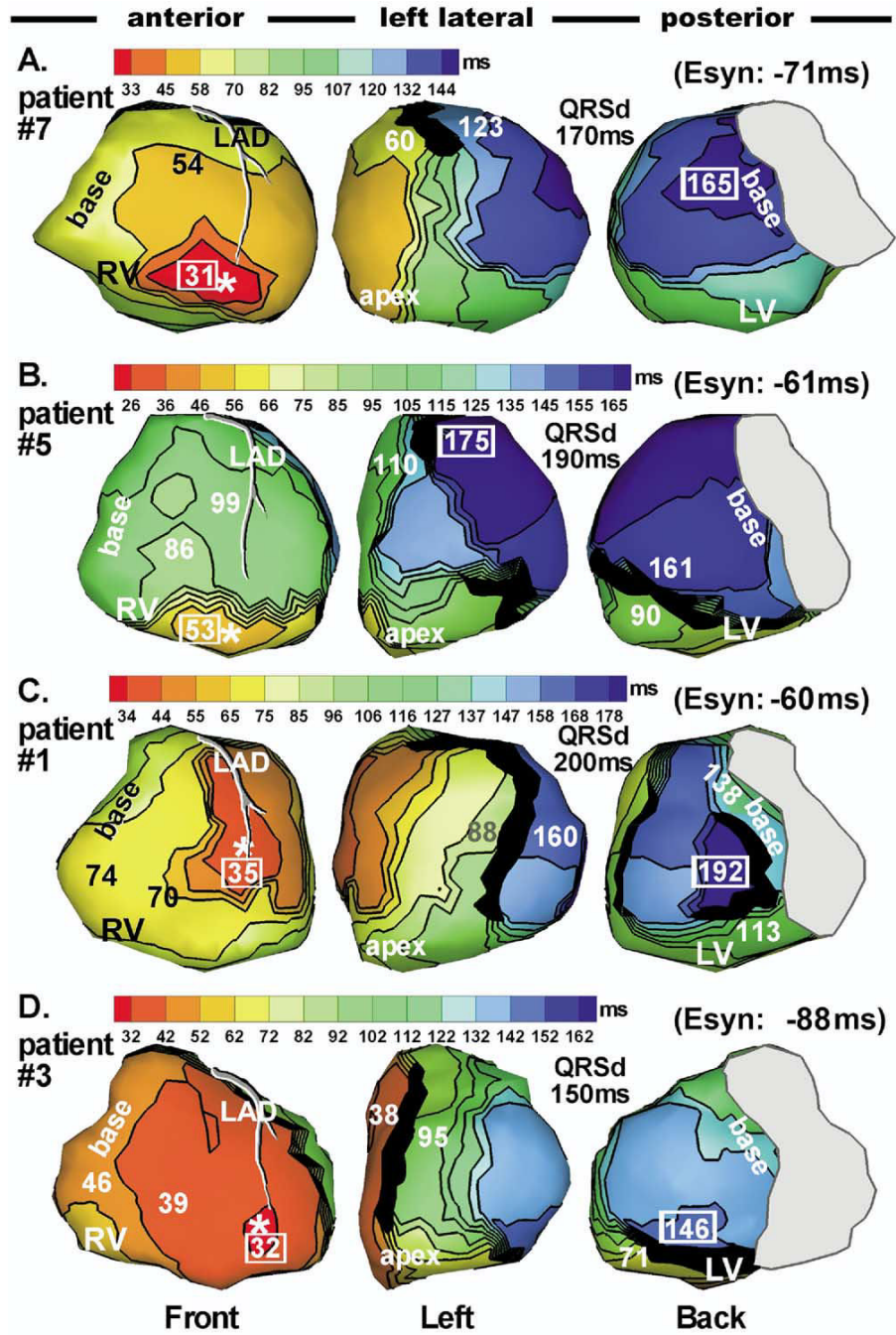


Figure 2. Isochrone maps during right ventricular (RV) pacing with optimal atrial-ventricular delay (AVD) in the same patients shown in Figure 1 (same format). Pacing site is indicated by an *asterisk*. All activation times are given with respect to the pacing stimulus.

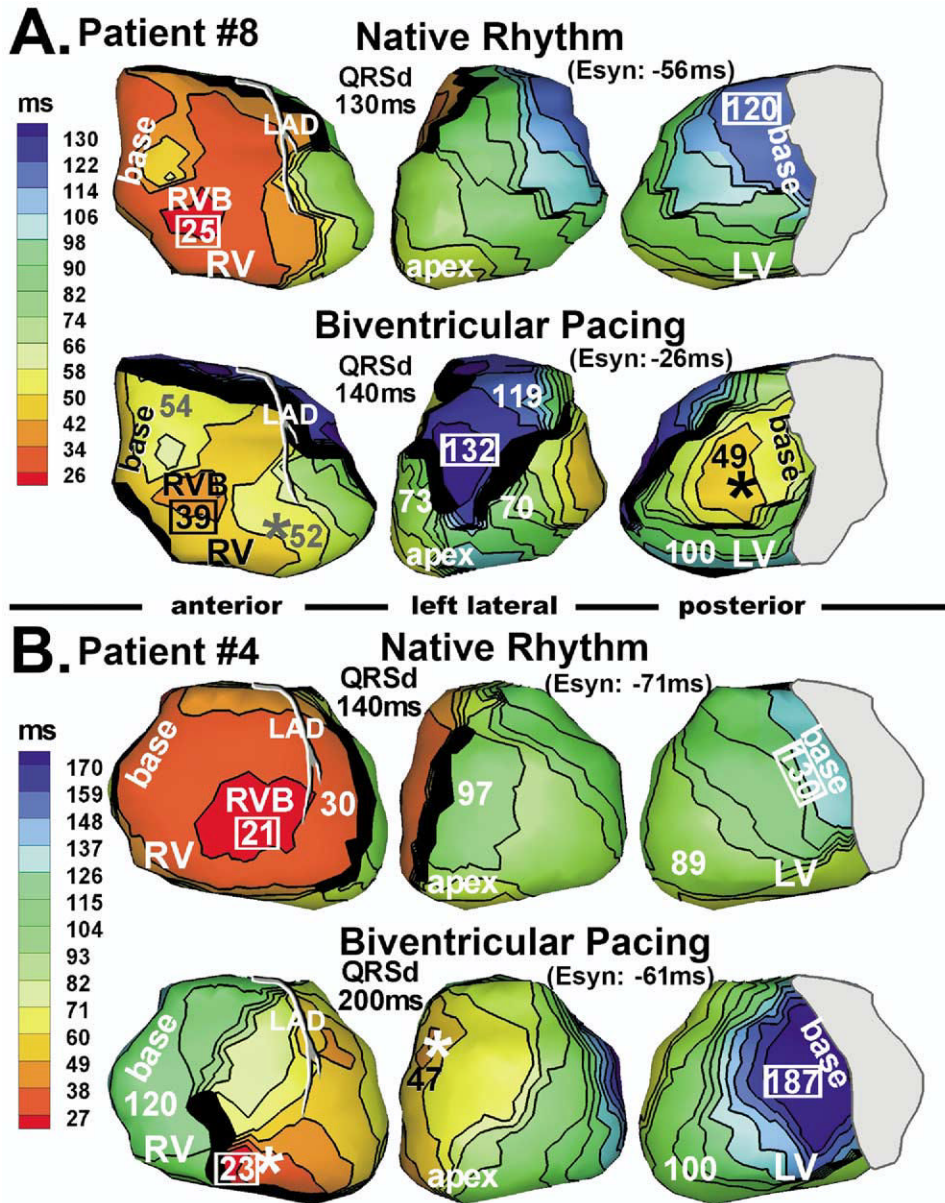


Figure 4. Isochrone maps during native rhythm and biventricular pacing. **A:** Patient 8. **B:** Patient 4. Marked conduction slowing occurred on the left ventricle during pacing.

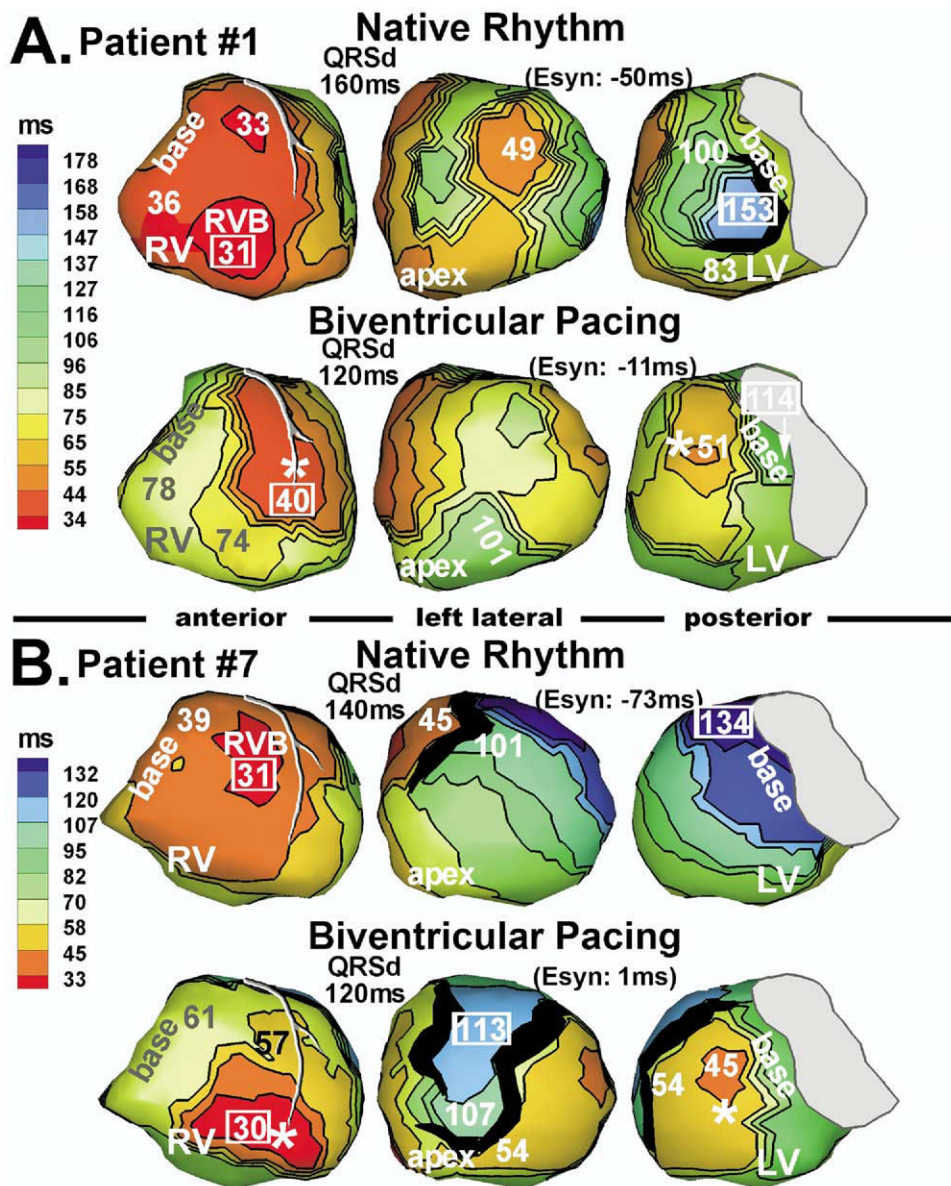


Figure 5. Isochrone maps during native rhythm and biventricular pacing. **A:** Patient 1. **B:** Patient 7.

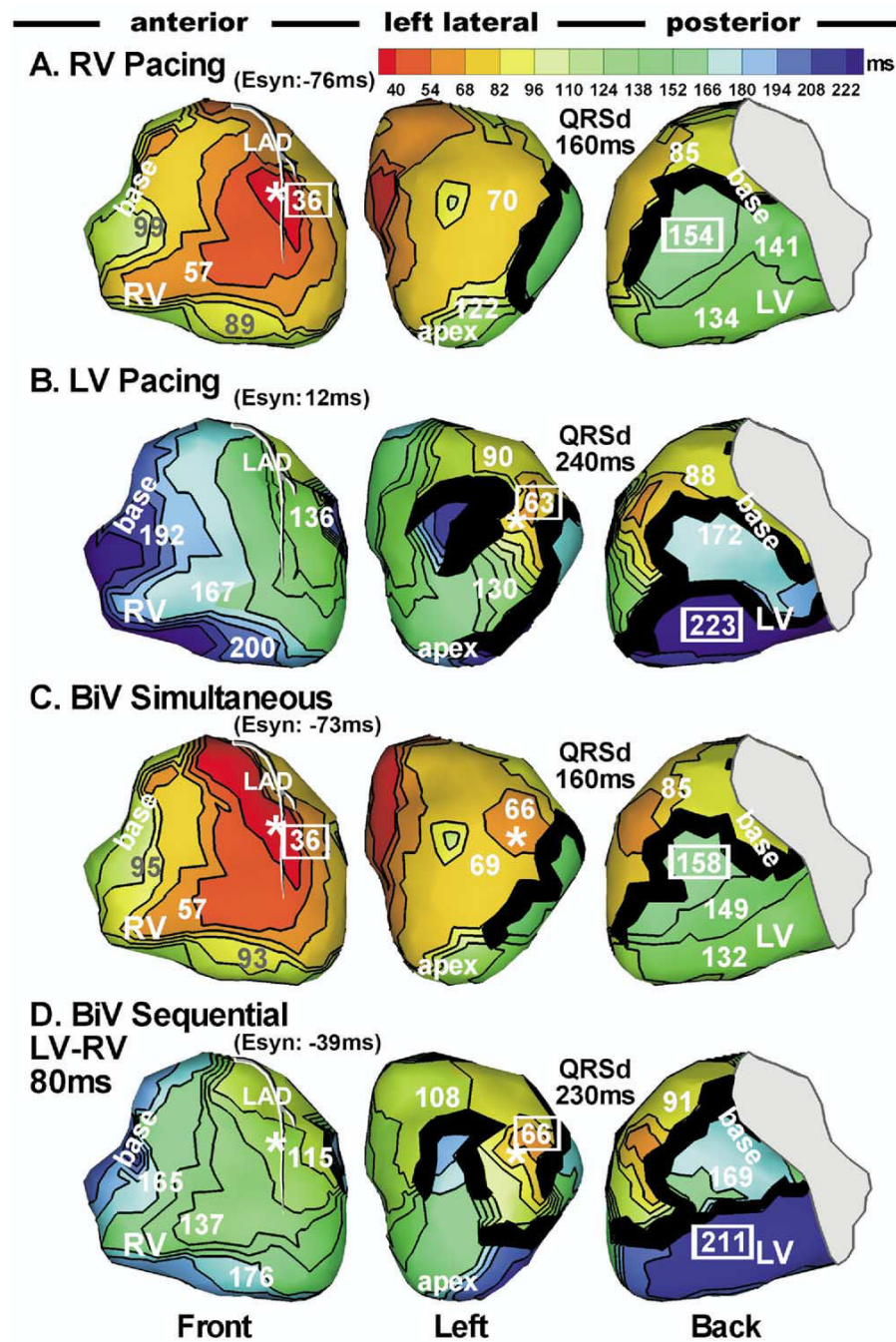


Figure 6. Sequential ventricular pacing. Isochrone maps during right ventricular (RV) pacing (A), left ventricular (LV) pacing (B), simultaneous pacing (C), and sequential biventricular pacing (D) in patient 6. During sequential pacing, LV is paced 80 ms earlier than RV.

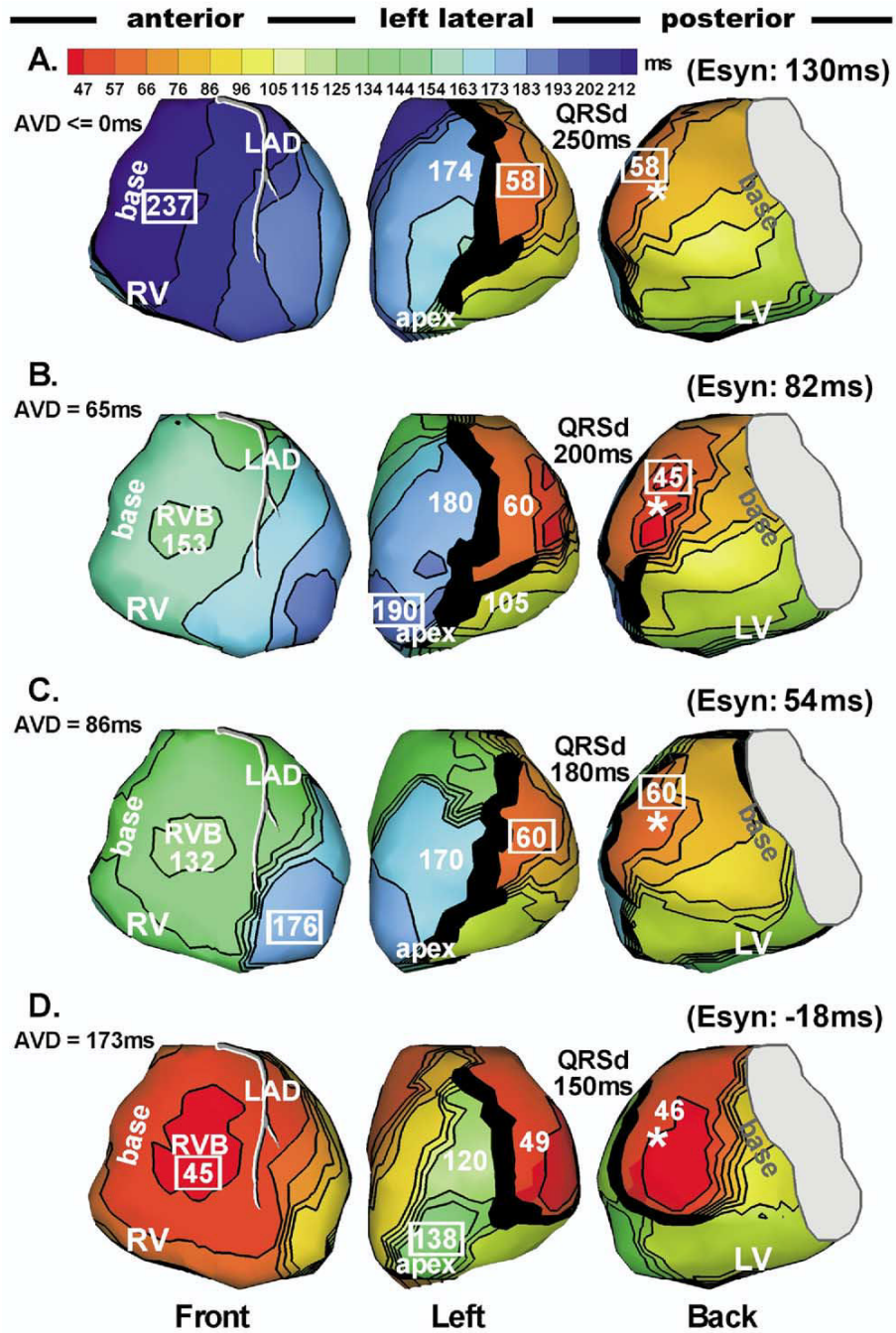


Figure 7. Fusion beats during left ventricular (LV) pacing. Isochrone maps during LV pacing in patient 5. Same format as Figures 1 and 2. **A:** LV paced activation sequence without fusion. **B–D:** Fusion beats with progressively earlier intrinsic right ventricular (RV) activation (time of RV breakthrough) relative to LV pacing as a consequence of increasing atrial-ventricular delay (indicated in each panel). Earlier intrinsic activation results in greater degree of fusion. **B:** Right ventricular breakthrough at 153 ms after LV pacing. **C:** RV breakthrough at 132 ms after LV pacing. **D:** RV breakthrough at 45 ms after LV pacing.

Table 1

Patient information

| Patient no. | Gender | Etiology | Response to CRT | Time of ECGI study (postimplant) | Underlying rhythm | LV lead location | Postimplant | | | | | | | | | | |
|-------------|--------|----------|-----------------|----------------------------------|-------------------|------------------|------------------------------------|-----------|----------|---|--|--|--------------------------|----------|---|--|--|
| | | | | | | | PR or atrial-ventricular delay(ms) | QRSd (ms) | LVEF (%) | LV internal diameter at end-diastole (cm) | LV internal diameter at end-systole (cm) | Biventricular optimal atrial-ventricular delay(ms) | QRSd(ms) (biventricular) | LVEF (%) | LV internal diameter at end-diastole (cm) | LV internal diameter at end-systole (cm) | |
| 1 | M | ISC | R | 40 d | SR | Lateral | | | | | | | | | | | |
| 2 | M | ISC | Non-R | 8 mo | No | Anterior | | | | | | | | | | | |
| 3 | F | ISC | R | 20 d | SR | Anterior | | | | | | | | | | | |
| 4 | M | IDC | Non-R | 7 mo | SR | Anterior | | | | | | | | | | | |
| 5 | M | ISC | R | 1 yr | SR | Lateral | | | | | | | | | | | |
| 6 | F | ISC | Non-R | 5 mo | AF | Anterior | | | | | | | | | | | |
| 7 | M | ISC | Non-R | 5 mo | SR | Lateral | | | | | | | | | | | |
| 8 | M | IDC | Non-R | 15 mo | SR | Lateral | | | | | | | | | | | |

| NYHA class | PR or atrial-ventricular delay(ms) | QRSd (ms) | LVEF (%) | LV internal diameter at end-diastole (cm) | LV internal diameter at end-systole (cm) | NYHA class | Postimplant | | | | |
|------------|------------------------------------|------------------|----------|---|--|------------|--|--------------------------|----------|---|--|
| | | | | | | | Biventricular optimal atrial-ventricular delay(ms) | QRSd(ms) (biventricular) | LVEF (%) | LV internal diameter at end-diastole (cm) | LV internal diameter at end-systole (cm) |
| III | 210 | 160 | 20 | 6.7 | 5.4 | II | 180 | 120 | 20-30 | 4.9 | 4.2 |
| IV | 200 dual-chamber | 220 dual-chamber | 10 | 8.2 | 7.2 | II | 140 | 170 | 10 | 9.5 | 8 |
| III | 160 | 180 | 25-30 | 5.2 | 4.6 | I | 160 | 120 | 30-40 | 5.6 | 3.4 |
| III | >300 | 140 | 15 | 8.2 | 7 | IV | 130 | 200 | 10-20 | 8.0 | 7.0 |
| III | 195 | 180 | 25 | 6.5 | 5.4 | I | 130 | 150 | 40 | 5.8 | 4.8 |
| III | N/A | 162 dual-chamber | 30 | 5.2 | 3.4 | IV | N/A | 230 | 30-40 | 5.7 | 4.2 |
| III | 160 | 140 | 15-20 | 6.0 | 5.1 | III | 130 | 120 | 20-25 | 6.2 | 5.3 |
| III | 140 | 130 | 15-20 | 6.7 | 5.2 | III | 130 | 140 | 20-25 | 7.1 | 5.3 |

AF = atrial fibrillation; CRT = cardiac resynchronization therapy; ECGI = electrocardiographic imaging; IDC = idiopathic dilated cardiomyopathy; ISC = ischemic heart disease; LV = left ventricular; LVEF = left ventricular ejection fraction; Non-R = nonresponder; NYHA = New York Heart Association; PR = PR interval; QRSd = QRS duration; R = responder; SR = sinus rhythm.

Table 2
Summary of electrical results during native rhythm, right ventricular pacing, and biventricular pacing

| Patient no. | Response to CRT | Native rhythm | | | | Right ventricular pacing | | | | Biventricular pacing | | | | | | |
|-------------|-----------------|----------------------|-----|------------|------|--------------------------|-----|------------|------|----------------------|-----|------------|------|-----|-----|-----|
| | | Mean activation time | | Figure no. | QRSd | Mean activation time | | Figure no. | QRSd | Mean activation time | | Figure no. | QRSd | | | |
| | | RV | LV | | | RV | LV | | | RV | LV | | | | | |
| 1 | R | 40 | 90 | 1C, 5A | -50 | 160 | 2C | 70 | 130 | -60 | 200 | 5A | 68 | 79 | -11 | 120 |
| 3 | R | 51 | 144 | 1D, 3B | -93 | 180 | 2D | 36 | 124 | -88 | 150 | 3B | 42 | 87 | -45 | 120 |
| 4 | Non-R | 30 | 101 | 4B | -71 | 140 | N/A | | | | | 4B | 69 | 130 | -61 | 200 |
| 5 | R | 29 | 141 | 1B, 3A | -113 | 180 | 2B | 88 | 149 | -61 | 190 | 3A | 88 | 68 | 20 | 150 |
| 6 | Non-R | N/A | | N/A | | | 6A | 63 | 139 | -76 | 160 | 6C | 61 | 134 | -73 | 160 |
| 7 | Non-R | 38 | 111 | 1A, 5B | -73 | 140 | 2A | 64 | 135 | -71 | 170 | 5B | 60 | 59 | 1 | 120 |
| 8 | Non-R | 32 | 88 | 4A | -56 | 130 | N/A | | | | | 4A | 52 | 78 | -26 | 140 |

All units are given in milliseconds.

Time 0 is the beginning of QRS complex for native rhythm and ventricular pacing stimuli for pacing episodes.

Mean activation time is average of activation times of 50–70 sites distributed over the lateral epicardial surface of the respective ventricle.

CRT = cardiac resynchronization therapy; Esyn = RV – LV mean activation time; LV = left ventricle; Non-R = nonresponder; QRSd = QRS duration; R = responder; RV = right ventricle.

Table 3

Substrate characterization

| Patient No | Substrate and motion abnormalities | Location of line of block (detected by ECGI) | | |
|------------|--|--|--|---|
| | | Figure no. | Native rhythm | Biventricular pacing |
| 1 | Posterior or inferior of the heart were extensively scarred and noncontractile; anterior anteroseptal, anterolateral hypokinesis; akinesis of the basal-midinferoposterior wall, basal-midposterior wall | 1C, 5A | Basal lateral LV, slow conduction in anterior LV | No |
| 2 | Anterior and anterolateral scarring; motion abnormalities in the inferior, posterior, lateral, anterior, septal, and apical walls | N/A | N/A | Anterior LV |
| 3 | Akinesis with scarring of the entire inferoposterior wall; most septum was infarcted along with the inferior wall | 1D, 3B | No | Anterolateral LV |
| 4 | Severe hypokinesis of the apical wall | 4B | Anterior LV | Anterior RV, slow conduction in lateral LV Anterior LV |
| 5 | Fixed anteroseptal, apical, inferior defects; anteroseptal/apical akinesis; inferior and posterolateral severe hypokinesis | 1B, 3A | Anterior LV | Anterior and lateral LV |
| 6 | 30-year-old large inferoapical and lateral myocardial infarction; inferoposterolateral and apical akinesia | 6 | N/A | Anterior and lateral LV |
| 7 | Scar involving the posterior inferior wall; small scar at apex; ischemia within the distal inferior wall | 1A, 5B | Anterior LV | Anterior LV |
| 8 | Akinesis of the entire posterior wall; severe hypokinesis of the basal inferoseptal wall; akinesis of the middistal inferoseptal wall; hypokinesis of the basal-midinferior wall | 4A | Anterior LV | Anterior and anterolateral LV |

ECGI = electrocardiographic imaging; LV = left ventricle; RV = right ventricle.